Insulator-to-superconductor transition in ultrathin films

Y. Liu,* D. B. Haviland,† B. Nease, and A. M. Goldman
Center for the Science and Application of Superconductivity and School of Physics and Astronomy, University of Minnesota, Minneapolis, Minnesota 55455
(Received 30 June 1992; revised manuscript received 18 November 1992)

The thickness dependences of the electrical conduction and the onset of superconductivity have been studied in ultrathin films of Bi, Pb, and Al. Thickness was varied by repeated *in situ* deposition of small increments of material onto amorphous Ge substrates held at low temperatures in an ultrahigh-vacuum environment. The thinner films of the resultant sequences of films were insulating and as thickness increased with successive depositions, superconductivity eventually appeared. This insulator-to-superconductor transition has been interpreted as a quantum phase transition, and compared in its features with predictions of the boson Hubbard model. The conductances of the sequences of films were scaled with a single parameter, and a universal scaling function was found. The scaling parameter vanished as the transition was approached from either the insulating or the superconducting side, falling as a power law of the difference between the Boltzmann conductance and a critical value of the conductance very close to $(h/4e^2)^{-1}$, or the inverse of the quantum resistance for pairs. The asymptotic value of the scaling function was also close to $(h/4e^2)^{-1}$, although this value was achieved only for Bi films. In the case of Pb and Al films superconductivity nucleated before the asymptotic limit was reached, at lower values of the conductance.

I. INTRODUCTION

Under conditions in which thermal fluctuations are suppressed, such as by cooling to low temperatures, the behavior of some macroscopic systems is dominated by quantum fluctuations. These may bring about quantum phase transitions, similar to thermodynamic transitions, but which are controlled by parameters other than temperature. It is believed that the disorder-driven insulator-to-superconductor transition in the limit of two dimensions and zero temperature is such a transition.[1]

Ultrathin films of various metals are important realizations of disordered electronic systems in reduced dimensions, and are good candidate systems for the study of the insulator-to-superconductor transition. Among the different types of material systems that have been investigated in this and related contexts, are high-temperature superconductors,[2,3] intermetallic compounds such as amorphous MoGe (Ref. 4) and MoC, (Ref. 5), amorphous-composite In-In_2O_3, (Ref. 6) and metals grown by deposition onto substrates held at liquid-helium temperatures (quench-condensed films).[7,8] The study of electrical transport of the latter has been carried out for almost fifty years beginning with the pioneering work of Shal'nikov[9] and Buckel and Hilsch.[10] Such "quench-condensed" films are inherently disordered. They exhibit insulating rather than metallic behaviors when the sheet resistance is sufficiently high. As it is reduced, they become either metallic or superconducting, depending on the evaporant. The sheet resistance is effectively a measure of the disorder of a film, and its value is directly controlled by thickness.

The investigations of ultrathin quench-condensed films deposited onto amorphous Ge (*a*-Ge substrates, which are presented here, were motivated by the goal of understanding the nature and the relationship between the distinct and essentially antithetical behaviors of the insulating and superconducting states of these films. The results of this work, which suggest the existence of a direct insulator-to-superconductor transition in the $T \rightarrow 0$ limit, are an important challenge to the conventional theory of the interplay of localization and superconductivity, and have in part motivated the development of the boson Hubbard model as a description of such systems.[1]

In high-resistance films, electrons are spatially localized, either as a consequence of the random potential, which leads to Anderson localization, or of interactions, which result in a Mott insulator, or a combination of both. For such films, the direct-current (dc) electrical conductance vanishes at zero temperature as a consequence of the localization of the electronic wave functions.[11] This localized state is gauge invariant.[12] In the opposite limit, the case of superconducting films, electrons move in a coherent manner over the entire sample. The dc resistance of the sample vanishes due to the quantum coherent character of the electron motion, and the ground state is characterized by the breaking of both the global and local gauge symmetry, which results in the well-known Anderson-Higgs phenomenon through the coupling of the matter and gauge fields.[13]

There are a number of questions that arise when one considers the interplay between superconductivity and localization. For example, can a superconducting state be constructed from localized single electron wave functions, or if the single electron wave functions are localized, must the system be insulating at zero temperature? In two dimensions, this issue becomes particularly intriguing as the lower critical dimensions for both localization and superconductivity are two. Superconductivity, i.e., zero dc resistance, is strictly possible only at zero

temperature.[14] Also, in two dimensions all electrons are believed to be localized even for the smallest possible levels of disorder.[11] As a consequence, it would appear that *either* insulating or superconducting states are allowed at zero temperature in two dimensions. Any transition between these two states, would be associated with a gauge symmetry breaking, and would be of fundamental interest.

The suppression of the transition temperature in disordered superconductors by the enhancement of Coulomb repulsion in the presence of weak disorder has been calculated using perturbation theory.[15,16] A consequence of this approach is that superconductivity can be weakened with increasing disorder even in the absence of scattering, which breaks time-reversal symmetry, as would be required by Anderson's theorem.[17] The calculated suppression of the mean-field transition temperature is in reasonably good agreement with the data, especially for low-resistance films.[4,5] These considerations have been extended to a more highly disordered regime using perturbative renormalization-group techniques, and somewhat better agreement with experiment has been found.[18] It should be noted that this approach is not applicable to systems in which disorder is strong, and, since it only accounts for the effect of disorder on the amplitude of the order parameter, it may not actually describe the demise of superconductivity, i.e., the appearance of resistance. The latter is connected with the breaking of long-range phase coherence, which may occur even when the order parameter amplitude is nonzero. Long-range or quasi-long-range phase coherence of the order parameter is directly responsible for the dc resistance vanishing, or the conductance diverging, which usually defines superconductivity.

In interpreting measurements on real systems it is necessary to note the importance of length scales in determining physical properties and the applicability of various models. Films of metals have conventionally been grouped into two extreme categories depending on the characteristic length scale of the disorder. Those with disorder on length scales substantially larger than atomic lengths, but much smaller than the sample size have been considered to be granular films, while films believed to have atomic scale disorder have been considered to be homogeneous. The physical models used to describe these extreme limits are nominally very different. These geometrical lengths must also be compared to those associated with localization or superconductivity. In the localization problem, one must distinguish between the strongly- and weakly-disordered regimes. In the weakly-disordered regime, the localization and the dephasing lengths are relevant.[19] The first determines the spatial decay of an electronic wave function, and the second, how far an electron propagates without losing phase memory assuming diffusive motion. At nonzero temperatures, the dephasing length cuts off the quantum interference effect, which is the essence of weak localization. Granular films and atomically disordered films are similar in the weakly-disordered limit, as the localization length is usually larger than the average grain size, at least in the two-dimensional limit.[19] In the strongly-disordered regime, electronic conduction is via thermally activated hopping processes. At sufficiently low temperatures, the competition between the probability for tunneling localized sites and thermal activation, controlled by the Boltzmann factor, gives rise to variable-range-hopping conduction,[20] with the optimal hopping distance being the important length scale. When superconductivity is involved, the superconducting coherence length, or the correlation length of the order parameter, is needed to characterize the system. This length must be compared with the length scale for disorder to determine the relevant physics. For example, when the superconducting coherence length of a granular film is sufficiently larger than the average grain size, the distinction between granular and homogeneous films should vanish.

Early studies of quench-condensed films were focused on understanding material properties that were different from those of bulk crystalline materials, such as the elevation of superconducting transition temperatures,[21] on superconducting fluctuation effects,[22] and on the issue of topological phase transitions.[23] A systematic experimental study of disordered superconducting films including films in the strong-disordered regime was carried out in 1970.[7] In this work, the films were prepared by successive deposition, *in situ,* onto substrates held at low temperatures. The superconducting transition temperature T_c was found to be a well-defined function of normal sheet resistance R_N, which was in turn controlled by the film thickness d. In effect, R_N is a convenient measure of the amount of disorder. Moreover, the values of T_c decreased monotonically with increasing R_N. In addition to the above findings, it was observed that extremely thin, and electrically continuous films, could be grown on substrates that were coated with thin layers of an appropriate material, such as a-Ge. In contrast, films grown directly on glass were initially connected electrically at much greater thicknesses. The former is the basis for the work reported here.

Differences between films grown directly on Al_2O_3 and glass substrates, and those grown on predeposited a-Ge underlayers have been noted in electron-tunneling studies.[8,24] It was observed that in the case of films grown directly on glass, which are considered to be granular films, the effective density of states depends on the normal sheet resistance only very weakly. On the other hand, for films grown on predeposited a-Ge underlayers, which are considered to be homogeneously disordered films, the effective density of states decreases monotonically with increasing normal sheet resistance R_N. Furthermore, for the latter, the ratio of the mean-field transition temperatures and effective densities of states remains approximately constant with increasing normal-state resistance. This implies that the decrease in T_c is a result of a reduction of the effective density of states at the Fermi surface. As T_c deceases, and the superconductor-to-insulator is approached, the energy gap also becomes small.[25]

In this work we will elaborate in detail the thickness dependence of electrical transport properties of homogeneously disordered films grown on a-Ge substrates.[26]

The results are very different from those of similar studies of granular films grown directly on glazed alumina or glass substrates.[27] In the latter, as thickness was increased, insulating, "locally superconducting," "metallic," and finally fully superconducting behaviors are observed in succession. In a locally superconducting film, as temperature decreased, the resistance first increases, and then at a temperature close to the transition temperature of the bulk crystalline form of the evaporant, the resistance falls to a local minimum. As temperature is reduced further the resistance continues to increase. The initial fall in resistance is interpreted as evidence of the onset of superconductivity within grains that are otherwise isolated or only weakly linked. The increase of resistance as temperature is decreased further is associated with the opening of a gap in the excitation spectrum of the grains, which results in an *increase* in the tunneling resistance between them. If the grains and the junctions coupling them are sufficiently small, then the charging energy is appreciable and the phase associated with the superconducting order parameter is strongly fluctuating, preventing the system from establishing a globally phase-coherent state. The term, "quasi-reentrance" has been used to describe plots of $R(T)$ exhibiting these local minima. Films with thicknesses close to the threshold for superconductivity, but which exhibit a nearly temperature-independent resistance at low temperatures are referred to as metallic. This phase presumably does not persist down to $T=0$.

Fully superconducting behavior in *granular* films was observed *only* after the normal sheet resistance of the films fell below a value which was close to $h/4e^2 (=6455\Omega)$, the quantum resistance for pairs.[27] In a series of experiments involving Sn, Al, Ga, and Pb films this value of the resistance threshold was repeatedly found, and would appear to be material independent. Granular films have been modeled as junction arrays, with zero resistance a consequence of the suppression of phase fluctuations, either by damping, or by renormalization of the intergranular capacitance to a larger and fluctuation-suppressing value by quasiparticle tunneling effects. The experimental results are unable to distinguish between the two approaches, although evidence from experimental work on ordered, low-capacitance, junction array systems supports the capacitance renormalization picture.[28]

In contrast with the above, films grown on *a-Ge substrates* exhibit much simpler behavior.[26] In the low-temperature limit, electrical conductivity either decreases or increases monotonically with decreasing temperature, and the more complicated phenomena described above are not observed. In modeling these films there are two important caveats: The first has to do with the role of the *a*-Ge substrates. The "conventional wisdom" is that the Ge underlayer only enhances the wetting of the substrate by the various metals. However, a case can be made that its role is much more complicated. Investigations on the Ag/Ge system demonstrate that Ge underlayers play a direct role in electrical transport.[29] This issue cannot be ignored in the case of Pb, Al, and Bi films deposited onto Ge underlayers. One *possible* scenario is that the structures of both "granular" and "homogeneous" films are actually granular. However, the grains of the films grown on *a*-Ge, which is an amorphous semiconductor with empty states, may be more strongly coupled electrically than those grown on glass or ceramic because of enhanced electron transport through the semiconductor.

The second caveat has to do with the possibility of quantum tunneling of Abrikosov vortices giving rise to finite voltages and nonvanishing resistances.[30] When vortices are pinned, the resistance is zero. However, they can be depinned, leading to nonzero resistance. One expects that in the limit of small current vortices would be pinned at sufficiently low temperatures. However, quantum tunneling of vortices[31] can bring about finite resistance even at zero temperature. An understanding of the role of tunneling and pinning would appear to be essential.

Experimentally, it may be difficult to decide whether a given film is truly superconducting. Although a definition based on the appearance of zero, or near zero, resistance is in principle unambiguous, it may not be very useful experimentally as in sufficiently disordered systems the transition temperature may be suppressed to a value below the accessible temperature range. Also, the measurement of very small voltages is limited by the sensitivity and noise levels of instruments. The study of another property of the superconducting state such as the energy gap, although of great interest, might not actually answer questions as to the disappearance of resistance, as a gap and a finite resistance can coexist. A similar difficulty exists for the insulating state, as there is always a nonvanishing conductivity due to thermal activation. Although one can use the temperature coefficient of resistance (TCR) at very low temperatures for specific samples to extrapolate to the zero-temperature limit, there are always dangers in such a procedure, and other ways of analyzing data are required to infer the behavior of the sample at the temperatures lower than those accessed experimentally.

This paper is organized in the following way: in Sec. II, experimental techniques are described. In Sec. III the data and scaling analysis of the conductivity of films of Bi, Pb, and Al grown on *a*-Ge substrates is presented and compared with results of a similar nature found for nonsuperconducting Pd films grown directly on ceramic substrates. In Sec. IV the relevance of the boson Hubbard model to the observed insulator-to-superconductor transition is considered. This model is a major advance beyond the theory of the interplay between superconductivity and localization in the description of the phenomenon being considered here. The various issues raised by this work are discussed in Sec. V.

II. EXPERIMENTAL PROCEDURES

The apparatus used in this study combined state-of-the-art ultrahigh-vacuum (UHV) and molecular beam epitaxy (MBE) technologies and low-temperature techniques. It provides the capability for *in situ* deposition of films and their measurement at low temperatures. Although the details of the apparatus have been described

in detail earlier,[32] a brief description will be included here for completeness.

The combination of MBE and low-temperature technologies was realized by attaching a stainless steel dewar, compatible with an UHV environment and equipped with a ^{3}He-evaporation refrigerator, onto the top of a MBE growth chamber. This chamber was pumped by two ion pumps (a 250-l/s differential ion pump and a 300-l/s conventional ion jump) with a total pumping speed of 550 l/s. The base pressure, which was measured and monitored with a residual gas being H_2. A Cu sample block was attached to the bottom of the ^{3}He-evaporation cell. The whole refrigeration unit was in turn attached to a flexible stainless steel bellows assembly, which allowed the sample block to be lowered into the growth chamber for the deposition of films and retracted back into the dewar for low-temperature measurements. The bellows assembly was welded to a gold-wire-sealed flange at its bottom end so that the sample block space was kept within an UHV environment at all times. Thermal shielding with liquid-nitrogen-cooled panels reduced the radiative heating of the sample during the deposition of a film. The metal vapor sources were commercial Knudsen cells (*K* cells). The crucibles were made of pyrolytic boron nitride and were approximately 13.8-cm deep and 1.8-cm inner diameter. The flux supplied from this type of crucible is substantially more uniform than that from ordinary Langmuir sources, which are usually crucibles or open thermal evaporation sources employing either tungsten or tantalum boats, wires or baskets. The *K* cells were heat-shielded by a hollow shroud through which cold air was flowed. This minimized outgassing from the *K*-cell units or the growth chamber walls. The pressure during growth remained below 1×10^{-8} Torr for even the highest operating temperatures of the sources, and was in the 10^{-9}–10^{-10} range for the deposition of metals. For the work described here, the highest temperature was about 1300 °C in the case of the deposition of Ge. For other materials, the cell temperatures, and operating pressures, as described above, were substantially lower.

Vapor fluxes were controlled by monitoring the source temperatures, which were measured using a thermocouple. The source temperatures remained constant during depositions. The amount of the material deposited was determined by the exposure time, which was controlled by tantalum shutters. These shutters were operated manually and could be easily opened for as short an interval as a few tenths of a second. This translated into a thickness increment of less than 0.01 Å. The source-to-substrate distance was approximately 45 cm.

Thicknesses were monitored using a quartz-crystal monitor. The crystal was mounted roughly parallel to the substrate and was about 6 cm away from the center of the film. The amount of material per unit area deposited on the crystal could be determined very accurately from the shift in its resonant frequency. The differences in the fluxes at the substrate and in the plane of the quartz crystal were accounted for by a calibration. This was obtained by depositing a thick Sn film at ambient temperature and determining the associated shift in the frequency of the monitor and correlating it with the film thickness as measured using a profilometer. However, the thicknesses reported in this paper are nominal in that standard bulk crystal densities were used to compute thicknesses from measured masses per unit area. Naturally, these densities might not be the same as those of the actual films (determining the latter would require detailed knowledge of film structure, which was not available). Additional error may be introduced as the quartz crystal was not kept at an absolutely constant temperature. Thermal drift could be significant for sources that were operated at high temperatures. However, the thermal response of the crystal could be distinguished from its response to mass by waiting for the source to return to equilibrium after a deposition before recording the frequency shift.

The films were grown on glazed alumina (99.% Al_2O_3) substrates, which were 2.54-cm square and 0.625-mm thick. The glaze, which was a 0.013-cm thick layer of Al_2SiO_3 provided an extremely smooth surface. The substrate were mechanically pressed onto the sample block. A small amount of Apiezon N grease mixed with fine Cu powder was applied between the unglazed face of the substrate and the sample block surface to enhance the thermal contrast between the substrate and sample block. The films were patterned to permit four-point probe measurements. A very uniform magnetic field could be applied in a direction perpendicular to the plane of the films using a split-coil superconducting magnet. Due to the size of the magnet, and the limited current carrying capacity of the electrical leads, the maximum value of the magnetic field was limited to about 2100 G. The uniformity of the magnetic field was $\pm1.1\%$ in a 1-cm diameter spherical volume. Samples could be aligned to within 0.5 cm of the center of the magnet.

Film resistances were measured using both dc and ac techniques. Electrical contacts were provided by wires connected to preevaporated 5000-Å-thick Ag pads. These pads were in turn connected to 100-Å-thick leads deposited after the substrate was loaded into the UHV chamber. These leads provided contact to the ultrathin films. For films involving a Ge underlayer, which was deposited *in situ* as well, all the layers were connected to the leads since the Ge layers were never more than about a monolayer thick and electrons could easily move through this thickness of Ge. The films were 0.5 mm$\times$5.0 mm in area, or ten squares. Current was supplied by a Keithley model 220 Programmable dc current source and the voltage was measured using a Kiethley model 181 nanovoltmeter. ac measurements were carried out using a PAR-124A lock-in amplifier. On some occasions, a transformer was used to match the impedance of a film to that of input amplifier of the lock-in amplifier in order to achieve the best noise figure. Temperatures were measured and controlled using a Quantum Design Digital R/G Bridge. Data acquisition was controlled and managed by an Apple II^+ computer through an IEEE interface bus. The lowest and highest temperatures for the measurements were 0.44 and 14. 2 K, respectively.

All low-temperature measurements were performed within a metal dewar, and all electrical leads entering the vacuum chamber were filtered with low pass electromag-

netic interference filters (Erie #1233-006), which were soldered into a conductive shield. In series with these filters, inside the shield, were 20 nH inductors. The combination of filters and inductors exhibited voltage attenuations of 15 dB at 1 MHz, 60 dB at 10 MHz, and finally 75 dB beyond 100 MHz. However, there were no low-temperature filters so that room-temperature thermal noise generated in the leads inside the apparatus could have in principle affected the sample.

The surface quality of the substrate is obviously crucial to the growth of ultrathin films. Given the fact that the setup was not enclosed in a clean room, extreme care was taken to clean the substrate beforehand and to keep it clean in subsequent handling in which it was loaded into the cyrostat. Substrates were cleaned ultrasonically first using acetone and then with methanol. The 5000-Å-thick Ag pads were evaporated in a separate small vacuum chamber. Jumper wires were attached to connect to the parts to the printed circuit board, which was in turn connected to the instruments. For films of Bi, Pb, and Al, these wires attached by direct soldering. Later, a technique using Ag epoxy was adopted for films of Ag and Pd. This technique was not nearly as labor intensive as the previous one. Substrates were always kept in a closed case in between various steps so as to avoid dust landing on their surfaces. After finishing these preparations, substrates were washed with methyl alcohol and dried using Omit-Plus lint and dust remover, before enclosing them in the system. These procedures for preparing substrates were found to be adequate in order to obtain connected ultrathin films.

The unique feature of the apparatus was that it could be used to successively deposit material and measure properties of films *in situ* at low temperatures. A sequence of films was fabricated and measured in the following way: A certain amount of material was deposited and then the sample block was retracted into the cyrostat for resistance measurements. The cryostat chamber was separated by two optically tight doors, which were held at liquid-nitogen and liquid-helium temperatures, respectively. The pressure in cryostat chamber was significantly lower than that in the growth chamber due to cryopumping. After the resistance measurements, the substrate was again lowered into the growth chamber and more material was deposited on top of the existing film. The resultant film was then driven back into the cryostat for additional measurements. The temperature of a film was generally kept between 14–20 K during the deposition (for Bi and Pb films, the highest temperature was 18 K). At these temperatures the gases absorbed on the film were desorbed.

The procedure described above is illustrated in Fig. 1. This "layer-by-layer" approach to growing ultrathin films revealed detailed features of the evolution of the electrical conduction encompassing a range from strong to weak disorder as the thickness was increased semicontinuously. The operation of this system required a great deal of patience and persistance. A typical run involving a film sequence of a specific material could take up to a few months. During this time considerable care was needed to maintain the extremely stable operating conditions needed to keep the parameters of the films constant.

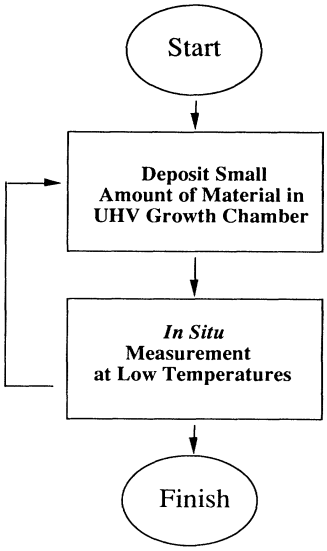

FIG. 1. Flow diagram of an experimental run for fabricating and measuring a sequence of ultrathin films.

Finally, it should be pointed out that there was no capability for structural analysis in this apparatus. Therefore, the morphology of the films was inferred only from transport measurements or from information on similar system found in the literature. As a result, definitive statements on film structure cannot be made.

III. DATA AND SCALING ANALYSIS

In this section, the results of studies of ultrathin films of superconducting materials will be described. Before doing this, it would be of value to review the properties of the three materials, Bi, Pb, and Al. Bismuth is an inherently very complex element. It is a pentavalent and possesses an atomic configuration given by $4f^{14}5d^{10}6s^26p^3$. When forming a bulk crystal, the five s- and p-electrons become conduction electrons, while the other electrons, which are strongly bound to the nuclei, are not relevant to transport processes. Crystalline Bi is a semimetal characterized by a very low carrier concentration. There are equal numbers of electrons and holes with concentrations of either being about $3\times10^{17}/\text{cm}^3$, a few orders of magnitude smaller than in ordinary metals (typically $10^{23}/\text{cm}^3$). The static dielectric constant of crystalline Bi is very high ($\kappa\approx100$). The crystal structure of Bi is a rhombohedral Bravais lattice with a two-atom basis. This is a layered structure with three electrons forming a strong covalent bond within each layer. The bonding between the layers, however, is of the van der Waals type, which is much weaker. It is important to note that the bulk crystalline Bi is not superconducting down to 0.05 K,[33] although small Bi grains have been recently reported to be superconducting.[34] When deposited at low temperatures, Bi forms an amorphous film with disorder on an atomic scale. The carrier density of amor-

phous Bi (a-Bi) is much higher than that of bulk crystalline Bi and has been measured to be $2.1\times10^{23}/\text{cm}^3$ assuming there are only electron carriers.[35] This indicates that a-Bi is a good metal. In addition, a-Bi is superconducting around 6 K.[36]

Lead is a heavy metal in the 4A column of the periodic table. In crystalline form, it becomes superconducting at 7.19 K. When deposited onto substrates held at liquid-helium temperatures, while not alloyed with a second metal, it does not form an amorphous phase unless it is grown at very low temperatures. However, the amorphous phase can be stabilized by adding a small amount of Bi. For $Pb_{0.75}Bi_{0.25}$, the superconducting transition temperature is 6.9 K and the measured carrier (electron) density is $2.84\times10^{23}/\text{cm}^3$.[37] It is worth noting that both Bi and Pb are heavy materials and therefore exhibit strong spin-orbit scattering. The spin-orbit coupling strength is typically proportional to Z^4, where Z is the atomic number. This may be important in the understanding the electrical conduction of these systems.

Aluminum is a metal in the 3A column of the periodic table. Its superconducting transition temperature is 1.196 K in pure form and can be significantly higher in the case of dirty samples or thin films. The carrier density measured for crystalline Al is $6.1\times10^{22}/\text{cm}^3$ (holes). Aluminum does not form an amorphous phase even when deposited onto substrates held at liquid-helium temperatures.

The a-Ge underlayers were grown with the substrates held at low temperatures, and Knudsen cells were used as vapor sources. Their thicknesses were 6.0 Å, 5.7 and 5.7 Å, respectively, for the particular sequences of Bi, Pb, and Al films described here. The sequence of Pb films exhibited a measurable conductance [$R(4\text{ K})<10$ GΩ] at the smallest thickness (2.4 Å) of the three. The Al films were considerably thicker when they became conductive.

The evolution of the conductivity of Bi films is illustrated in Fig. 2. Each individual curve represents a single film. The symbol G denotes the conductance in units of $4e^2/h$, i.e., $G=(h/4e^2)/R$, where R is the resistance per square. To avoid too high a density of data points, not all the data is included in this figure. Although the data are not explicitly shown, Pb and Al films behaved in a similar manner.[38]

A common feature of the data was its nature in the limit of zero temperature. Films were either insulating or superconducting, with those exhibiting conductance curves increasing with decreasing temperature considered to be superconducting and those with the opposite slope insulating. This categorization implies an extrapolation to temperatures below those actually reached experimentally. Nevertheless, general features of the data strongly support it. Also local superconductivity, as defined in Sec. I, was not observed. Its absence has been taken as evidence of a homogeneous structure with disorder on an atomic length scale. However, this is only indirect evidence, as studies of structure were not carried out.

In Fig. 3, the electrical conductances of the ten thinnest Bi films are plotted against temperature. In the $T\to0$ limit, these exhibit an Arrhenius form, i.e., $G=G_0\exp(-T_0^I/T)$. This is similar to "fixed-range-hopping" (FRH) conduction.[39] However, more careful examination of the data indicates that this temperature dependence may not be attributable to FRH. The prefactor G_0 is roughly independent of thickness, or sheet resistance at 14 K, as this is shown in Fig. 4. The value of G_0 is about 0.174, which corresponds to a conductivity $\sigma_0\approx0.11e^2/\hbar$, a result not expected from FRH picture. The number, $\sigma_0\approx0.11e^2/\hbar$, or $1/37k\Omega$, is very close to the "universal minimum metallic conductivity" in two dimensions, obtained in early theoretical studies predating the modern scaling theory of localization.[40] In that context, the data could be taken as evidence of a mobility edge separating the conduction and valence bands and the "minimum conductivity" would simply be a measure of the mobility right at the mobility edge. Correspondingly, T_0^I would be the measure of the mobility edge. Although the "minimum metallic conductivity" is believed not to exist in two dimensions as all electronic states are

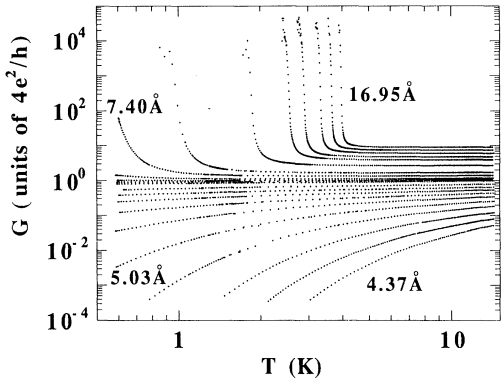

FIG. 2. Evolution for Bi films of the electrical conductance G in units of $4e^2/h$ as a function of temperature T. The thicknesses of a few selected films are indicated. Note that conductance and conductivity are identical in two dimensions. Only some of the data of the sequence of films is shown to avoid too high a density of data points.

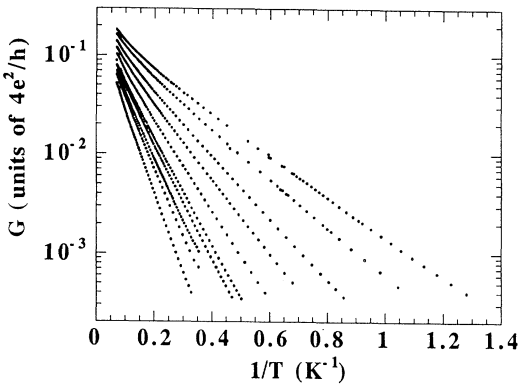

FIG. 3. G vs $1/T$ plotted on a semilog scale for the ten thinnest Bi films (the first to the tenth films of the Bi sequence). An Arrhenius law is clearly seen.

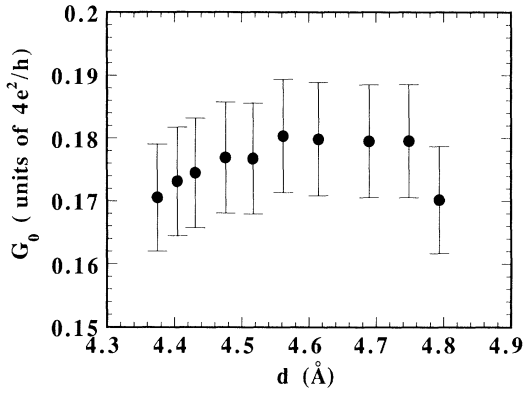

FIG. 4. The prefactor G_0 obtained by fitting an Arrhenius law to the data of G vs T of the ten thinnest Bi films. Error bars indicated were estimated from the variations in the fitting parameter G_0 in fitting over different ranges.

localized, this notion may still be a useful description of electron conduction at high temperatures. Of course if there were a real gap (i.e., hard gap) in the quasiparticle excitation spectrum, possibly associated with spin degrees of freedom,[41] then the prefactor G_0 would have a different origin.

As film thickness is increased, the electrical conductance deviates from Arrhenius behavior at low temperatures. Eventually, with sufficiently thick films this Arrhenius tail becomes very difficult to identify. For such films, plotting the logarithm of the conductances against $(1/T)^n$ with n as a variables suggests that the conductance in the low-temperature limit is best described as variable-range-hopping with a Coulomb gap, characterized by $G \sim \exp[T_0^I/T)^{1/2}]$.[42] This is shown in Fig. 5 where the values of G for the 11th through the 21st films are plotted.

As the thickness is increased even further, the conductance becomes logarithmic in temperature as shown in Fig. 6. This dependence, $G = G_B + B \ln T$, where G_B is the Boltzmann conductance and B is a number independent of temperature, is typical for electrons in the weak localization regime.[19] However, noticeable deviations from logarithmic behavior can be seen in the plot. They may be due to effects that have not been taken into account in the perturbation calculations, which are the basis for the weak localization theory. It is interesting to note that the slope of the logarithm in the low-temperature limit decreases as the onset of superconductivity is approached. The best fit to the data at low temperatures indicates that B varies from 9.72×10^{-2} for the 22nd film to 5.5×10^{-7} for the last insulating film.

Insulating films of Pb and Al behaved in a manner similar to those of Bi.[38] For the thinnest, the electrical conductance had the Arrhenius form, $G \approx G_0 \exp(-T_0^I/T)$. In contrast with the case of Bi, the prefactor G_0 for Pb and Al films, rather than being constant, depended on thickness. With increased thickness the conductance followed $G \sim \exp[(-T_0^I/T)^{1/2}]$ in the low-temperature limit. Finally, $G(T)$ was close to logarithmic in temperature for thicker films although significant deviations from logarithmic behavior, particularly in the low-temperature limit, were observed. These deviations made it difficult to fit the data with a logarithmic form.

The onset of superconducting behavior in the various sequences could be correlated with the value of the resistance in the normal state. In the case of films in the Bi sequence, there was a sudden drop in the resistance with decreasing temperature when the normal-state sheet resistance, measured at 14 K, fell below $R_0 = 6.42 \pm 0.2$ kΩ. This threshold value R_0 was taken as the algebraic average of the resistance measured at 14 K for the last insulating and the first superconducting films of the sequence, respectively. The quoted uncertainty was arbitrarily taken to be the order of the difference between the resistances of these two films at 14 K. It is very striking

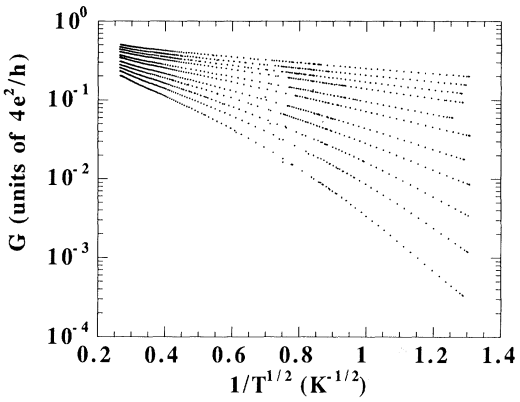

FIG. 5. Conductance G vs $1/T^{1/2}$ of the 11th to 21st films of the Bi sequence. These films are of "intermediate" thickness. In the low-temperature limit the conductance is best fit by the form predicted by a model involving variable range hopping with a Coulomb gap.

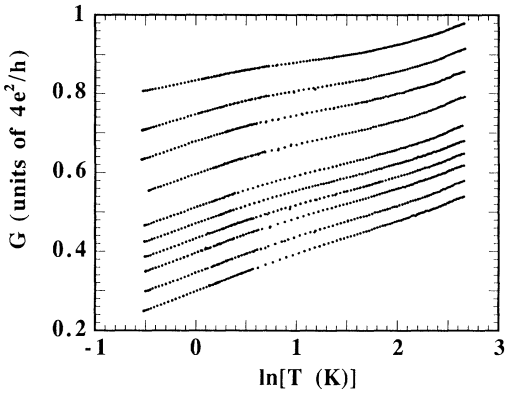

FIG. 6. Conductance G vs $\ln T$ of last ten insulating Bi films. (The 22nd to 31st films of the Bi sequence.) The temperature dependences of the conductances are approximately logarithmic. Notice that in the low-temperature limit, the slope of the logarithm decreases as the onset of superconductivity is approached.

that R_0 is close to the quantum resistance for pairs, $h/4e^2$(6455 Ω). Since there is a slight temperature dependence to the resistance even at high temperature [dR/dT(14 K)≈ -0.062 kΩ/K for the first superconducting film], the selection of 14 K as the temperature for the normal resistance is somewhat arbitrary. However, as will be shown later, this does not affect the conclusions in fundamental manner. The corresponding values of the threshold for Al and Pb, respectively, were (9.94±0.4)kΩ and (18.6±1.7)kΩ for Pb and Al. These results are shown in Fig. 7. It should be noted that among the three materials studied, the differences between the thicknesses of the last insulating and first superconducting films was smallest for the Bi sequence.

The resistances at high temperatures, even for superconducting Bi films, exhibited a small negative temperature coefficient of resistance ($dR/dT < 0$). A similar negative temperature coefficient of resistance was found in both the Pb and Al sequences. For Bi films, the negative temperature coefficient of resistance was found for *all* the films studied. For other two sequences of films, values of dR/dT at high temperatures gradually increased to zero and eventually changed sign with increasing film thickness. The physical origin of this sign change is unclear.

It is interesting to note that magnetic fields had a strong effect on the superconducting transition for films close to the threshold for superconductivity. In Fig. 8, the temperature dependences of the resistance of the first superconducting film in the Al sequence are plotted for different magnetic fields. The higher temperature data are not shown. Magnetic fields (< 1400 G) had negligible effects on film resistance at high temperatures. The flattening off, and also the apparent turning up of the resistance of this film are very similar to what has been observed in In-InO_x films where it was interpreted as magnetic-field driven superconductor-insulator transition.[43] This issue was not pursued in the work described here.

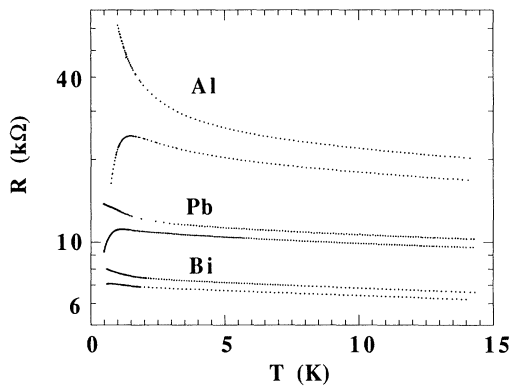

FIG. 7. Sheet resistance R vs T of the first superconducting and last insulating films for the Bi, Pb, and Al sequences. The algebraic mean R_0 of the resistance at 14 K of the last insulating and first superconducting films of the Bi, Pb, and Al sequences, respectively, are 6.42, 9.94, and 18.6 kΩ. These numbers are close to $h/4e^2$, $1.5(h/4e^2)$, and $3(h/4e^2)$, and appear to be system dependent.

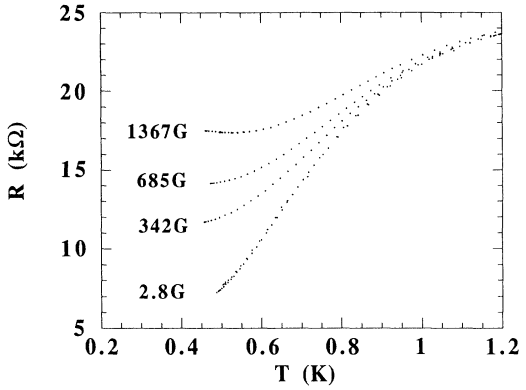

FIG. 8. Resistance R vs T in several magnetic fields for the first superconducting Al film in the Al sequence. In the highest magnetic field, the resistive tail levels off.

Another important feature of the films is the strong depression of the superconducting transition temperatures with decreasing thickness. Figures 9(a) and 9(b) contain plots of T_c vs $1/d$ and R(14 K), respectively. Here T_c is effectively the mean-field transition temperature, i.e., that temperature at which the resistance falls to half its value at $T = 14$ K. These data are in qualitative agreement with a number of models. Calculations based on the idea of an enhanced Coulomb repulsion in disorder films predict a reduction of T_c such as that observed.[15,16,18] However, for strongly-disordered films near the superconductor-insulator transition, such calculations should not apply. A second model involves the addition of a surface energy to the Ginzburg-Landau free energy, ignored in bulk systems,[44–46] and equivalent to a modification of the boundary condition for the order parameter. This will also impose a thickness dependence on T_c. A final possibility is the recent suggestion of Ferrell and Lobb that phase fluctuations are pair breaking.[47] This will lead to a reduction of the superconducting gap, and T_c with increasing sheet resistance.

It should be noted in passing, that for thicker Al films, small oscillations in T_c with thickness were observed. Similar behavior reported for granular Sn films grown on glazed alumina substrates, was attributed to a quantum size effect in a dimensionally constrained system.[48] For Bi and Pb films, such T_c oscillations were never found. These observations taken together may be related to the detailed structure of the various films, and will be the subject of future study.

A two-step drop of resistance developed in the low-temperature tails of the superconducting transitions of relatively thick Pb films. This suggests the presence of second superconducting phase with a transition temperature comparable to the first. The two phases could be the amorphous and crystalline phases of Pb. Another possibility is that one of them is associated with the Pb/Ge interface, being either a signature of interfacial superconductivity or an alloying effect. For Al films, similar features observed for thick films although effects directly

attributable to a distinct second phase could not be identified. The above-mentioned features of $R(T)$ of thick films in the Pb and Al sequences suggest the nucleation of chemical or/and physical inhomogeneities during the evolution of the sequence. It would appear that this did not happen in a detectable manner during the evolution of the Bi sequence. The possible reasons for these observations will be discussed in Sec. V.

The data for the Bi films shown in Fig. 2 can be scaled in an empirical manner. For insulating films, curves of G vs $\ln T$ of a given film can be shifted along the $\ln T$ axis to overlap with the film adjacent to it in the sequence. This operation can be applied successively to *all* insulating films of the sequence over the *entire* temperature range. Mathematically, this implies that the electrical conductance can be written in a scaled form, $G=G(T,d)=G(T/T_0^I(d))$, where d is the film thickness, and T_0^I is a characteristic parameter. The ratio of the values of T_O^I of two adjacent films can then be determined by the shift on the $\ln T$ axis required to overlap their plots of G vs $\ln T$. The value of T_0^I for the first film is determined by directly fitting the condensate data to the Arrhenius form. Then, starting with the vale of T_O^I for the thinnest film, values of T_0^I for each of the subsequent films can be determined by successive multiplication by the ratios of the scaling parameters for adjacent films. Once T_O^I is determined for each film, all of the data plotted as $G(T/T_0^I)$ collapses onto a single curve. This procedure worked over a wide range of conductances from the regime in which they were exponentially activated functions of temperature to that in which they were nearly logarithmic functions. It should be noted that Möbius used a similar procedure to collapse the conductance data of thick amorphous $Si_{1-x}Cr_x$ films with different values of the Cr context x.[49] This was done in the context of an attempt to prove the existence of a minimum metallic conductivity in three dimensions.

The outcome of the above procedure is illustrated in Fig. 10 in which values of G for 31 insulating films are plotted vs $\ln(T/T_0^I)$. The collapse of the data is very accurate, and there are only small deviations from scaling in the high-temperature limit for the films closest to the onset of superconductivity. To see this, the inset displays a linear plot of the data of Fig. 10. The inset also shows that for $0.2<G<0.8$ the scaling curve is very close to being a logarithm in T/T_0^I. It begins to level off as G is increased further.

The same analysis can also be applied to insulating Pb and Al films. The conductances for these two sequences are shown in Figs. 11 and 12, respectively. In both figures the collapse of the data is not as clean as it is for Bi. However, when all three sequences are plotted on the same graph, as shown in Fig. 13, they follow a *single* curve despite scatter of the data points for the Pb and Al films. It is important to note that values of T_O^I are determined independently for the three sequences of films without any adjustable parameters. The curve in Fig. 13

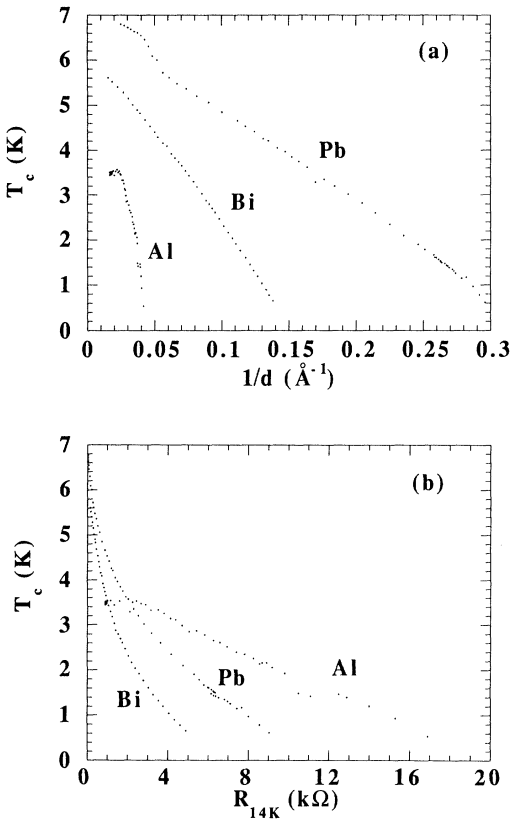

FIG. 9. (a) Superconducting transition temperature T_c, defined by $R(T_c)=R(14\text{ K})/2$, vs the inverse of the thicknesses $1/d$ for the Bi, Pb, and Al films. (b) Superconducting transition temperature T_c, defined by $R(T_c)=R(14\text{ K})/2$, vs $R(14\text{ K})$ for the Bi, Pb, and Al film sequences.

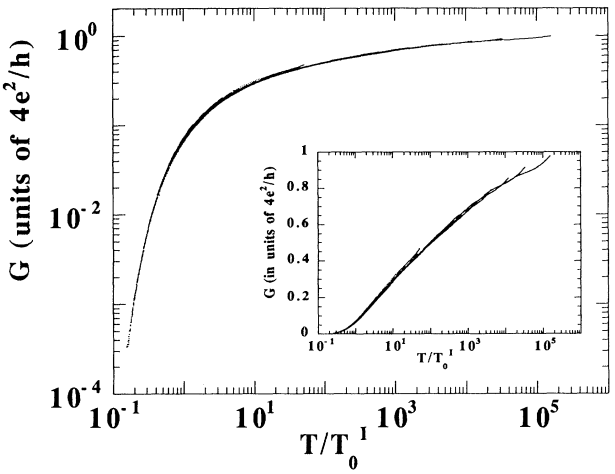

FIG. 10. Conductance G vs $\ln(T/T_0^I)$ for insulating Bi films in semilog scale. A linear plot of the same data is shown in the inset. Deviations from linearity are seen in the latter at high temperatures in the case of films with properties placing them close to the insulator-superconductor transition. An approximate logarithmic dependence on temperature is seen for films with $0.2<G<0.8$. For $G>0.8$ the scaling curve appears to level off.

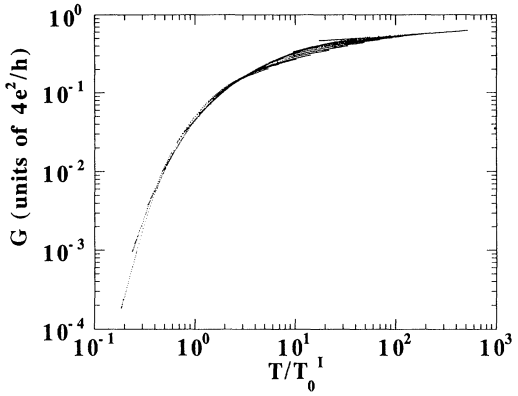

FIG. 11. Conductance G vs T/T_0^I for insulating Pb films.

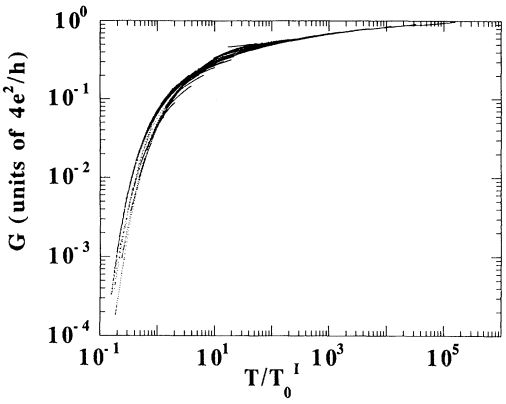

FIG. 13. Conductance G vs T/T_0^I for insulating Bi, Pb, and Al films. Note that values of T_0^I are independently determined for each sequence of films, without any adjustable parameters. This suggests that the scaling curve is universal, and therefore its asymptotic value is as well.

can be viewed as a general scaling function for the electrical conductances of insulating films of eventually superconducting materials. It has an Arrhenius form in the limit of $T/T_0^I \rightarrow 0$, i.e., for the thinnest films, and goes over to a form described as variable range hopping with a Coulomb gap ($\approx \exp[-(T_0^I/T)^{1/2}]$) in an intermediate range of thicknesses. As the value of T/T_0^I is further increased it becomes approximately a logarithmic function of reduced temperature. Finally in the limit of $T/T_0^I \rightarrow \infty$ the scaling curve tends to level off and *may* eventually become temperature independent.

Superconducting films with thicknesses near the crossover from superconducting to insulating behaviors were analyzed in an analogous manner employing a parameter T_0^S. It was found by shifting data of G vs $\ln T$, the low-temperature tails of the various conductance curves could be brought together to follow an envelop trajectory. For those films having sufficiently long conductance tails at low temperatures, the data also collapsed onto a single curve. Values of T_0^S were found by noticing that the low-temperature tails of film, which were superconducting, and at the same time close to the threshold for the transition to nonsuperconducting behavior, fell to zero as $\exp(-T_0^S/T)$. Using T_0^S of one of these films as a reference, values of T_O^S for the other films were determined without additional adjustable parameters.

However, in the analysis of data on superconducting films, the high-temperature conductance data does not actually collapse onto a single scaling curve. The values of the conductance of the first ten superconducting films of the Bi sequence are plotted vs T/T_0^S as determined by the above procedure in Fig. 14. In the case of thick Bi films, even further from the onset of superconductivity, the high-conductance tails overlap, but don't collapse onto a single scaling curve. Superconducting Pb and Al films could be analyzed in the same way.[38] The scatter of the data about the scaling function was quite noticeable even in the high-conductance limit for Pb films and deviations from scaling for Al films were substantial.

The scaling analysis presented above implies that the quantities $T_0^{I,S}$ are very important parameters of the system. In Fig. 15, values of both $\log_{10}T_0^I$ and $\log_{10}T_0^S$ for various Bi films are plotted as a function of the quantity $\delta_{14\,K}=R/R_0-1$, where R is the sheet resistance of a given film at 14 K, and $R_0=6.42$ kΩ is the average of the

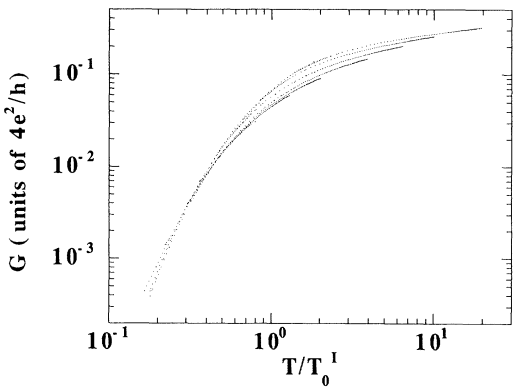

FIG. 12. Conductance G vs T/T_0^I for insulating Al films.

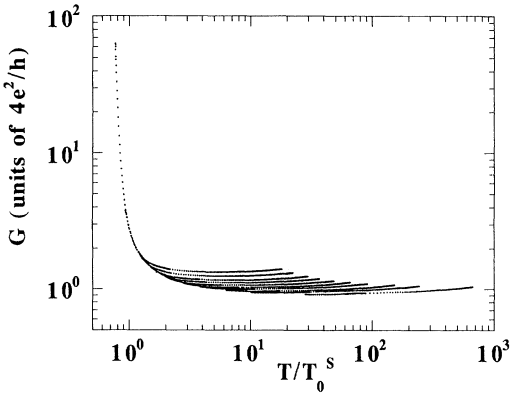

FIG. 14. Conductance G vs $\ln(T/T_0^S)$ for first ten superconducting Bi films.

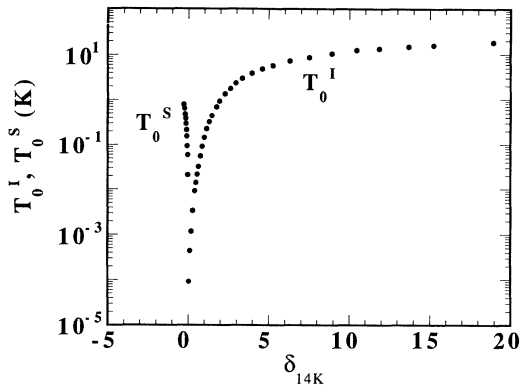

FIG. 15. Plots of T_0^I and T_0^S vs $\delta_{14\,K}=(R/R_0-1)$ for Bi films, where R is the sheet resistance at $T=14$ K and R_0 the average of the sheet resistances at 14 K of the last nonsuperconducting film and first superconducting film.

resistances of the last nonsuperconducting and first superconducting films of the sequence, also evaluated at 14 K. It is seen that both T_O^I and T_0^S fall abruptly to zero near $\delta_{14\,K}=0$. If thickness is used as a control parameter, a similar plot can be obtained.

A casual examination of Fig. 15, suggests that the limiting values of $T_0^{I,S}$ are proportional to $\delta_{14\,K}^{i,s}$ in the limit of $\delta_{14\,K}\to 0$. In this instance, the exponents i and s would be critical exponents of the insulator-to-superconductor transition. An approach to further analysis of the data would be to fit $T_O^{I,S}\sim\delta_{14\,K}^{i,s}$ to the data. From such a fit we find $i=2.8\pm0.4$ and $s=1.5\pm0.2$. This is illustrated in Fig. 16 in which plots of $[T_0^I]^{1/2.8}$ and $[T_0^S]^{1/1.5}$ vs $\delta_{14\,K}$ are shown. A similar analysis for the Pb and Al films is not all reliable because of significant scatter in the scaling curve.

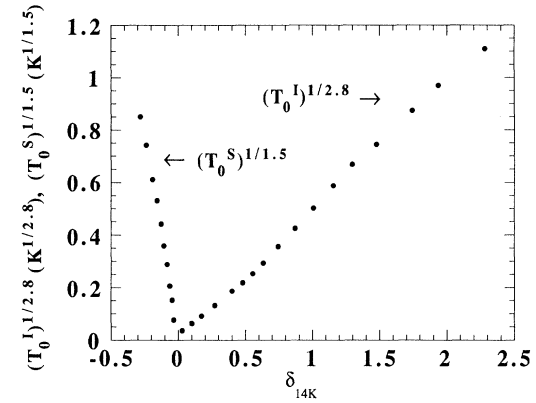

FIG. 16. Plots of $(T_0^I)^{1/2.8}$ and $(T_0^S)^{1/1.5}$ vs R for Bi films, where R is the sheet resistance measured at 14 K. Insulating films far from the insulator-superconductor transition are not included. It is seen that the data corresponding to the smallest values of T_0^I and T_0^S fall onto two separate straight lines. This implies an algebraic dependence of these quantities on the control parameter.

It should be noted that the resistance of the films, even at 14 K, is slightly temperature-dependent ($dR/dT<0$). However, this dependence is so weak for films close to the insulator-to-superconductor transition that the exponents resulting from the fit do not depend on the temperature at which δ is evaluated. If one chooses $\delta_{10\,K}$, with $R_0(10\text{ K})=6.62$ kΩ, and repeats the above analysis, the values of i and s turn out to be the same as those obtained using δ_{14K}, demonstrating that δ, as defined, is a reasonable choice for the control parameter of the transition.

The fact that the exponents i and s differ by a factor of 2 is unusual, but may be a reflection of intrinsic physics of the system which is unidentified at this time. However, it should be emphasized that there is always a danger in extracting critical exponents from experimental data obtained in a temperature range over which the system is not in the critical regime. Such may be the case in this instance. In Fig. 17, we show a $\log_{10}$-$\log_{10}$ plot of $T_0^{I,S}$ vs $\delta_{14\,K}$. This emphasizes limiting values for small $\delta_{14\,K}$, and demonstrates that the data are not yet up to the standards of studies of critical phenomena. If only the last data points for both superconducting and insulating films are considered, the exponents appear to *both* approach the superconducting value of 1.5, although the density of the data leaves the outcome uncertain. This important issue will be resolved in future studies in which extensive data at lower temperatures, and closer to the insulator-superconducting transition are obtained.

The success of the above one-parameter scaling analysis suggests that the values of resistance measured at high temperatures can be associated with those which would be obtained at zero temperature if the latter could be achieved experimentally. Starting from a film with a superconductor or insulator at $T=0$ according to the one-parameter scaling. (This is a more reliable approach to determining whether a film is an insulator or a superconductor than a simple extrapolation based on TCR.) Operationally, the scaling analysis permits the determination of the limiting resistance at zero temperature as it

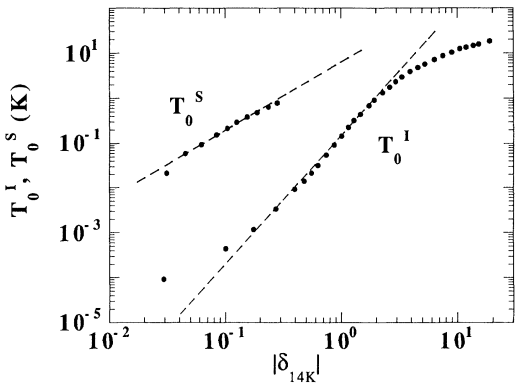

FIG. 17. Logarithms of T_O^I and T_0^S vs $\log_{10}|\delta_{14\,K}|$. The dashed lines are fits to $T_0^S\sim|\delta|^{1.5}$ and $T_0^I\sim|\delta|^{2.8}$ This plot emphasizes behavior near the critical point.

determines the scaling function, $G=G_{I,S}(T/T_0^{I,S})$. Although details for specific films may result in deviations from the scaling curve, the overall features and the asymptotic value of the scaling function appear to be universal.

The two asymptotic limits of the scaling function, $G_I(0)\rightarrow 0$ and $G_S(0)\rightarrow\infty$, correspond to the insulating and superconducting states, respectively. The asymptotic value, $G^*=G_I(\infty)=G_S(\infty)$ defines a critical resistance R_c. Given the accurate scaling of Bi films on the insulating side, the asymptotic limit of the scaling function is seen to be very close to $G^*=1(R_c=h/4e^2)$. Since the scaling curve is universal, so is its asymptotic limit. This leads to the conclusion that R_c defined in the above manner is a universal quantity. This conclusion does *not* contradict any previous experimental results obtained by any group. Unless the existence of this scaling curve is an accident, or there exists a different scaling curve with a different asymptotic value, the universality of the critical resistance defined in this manner would appear to be on firm ground.

It is important to distinguish this limiting resistance of the scaling function R_c from the threshold for the onset of superconductivity R_0 as defined earlier. The latter has been measured in this work for Bi, Pb, and Al films and also by others for various systems.[2,8] It appears that the two quantities may or may not coincide. For the set of Bi films they happen to have the same value. Incidentally, a search of the literature suggests that the values of the threshold for superconductivity R_0, may be very close to $n/2(h/4e^2)$ where n is an integer.[38] (For the Bi, Pb, and Al films of this work, the values of n are 2, 3, and 5, respectively).

It should be pointed out that the asymptotic value of the conductance can, in principle, be reached experimentally. As $T\rightarrow 0$, $T_O^{I,S}$ can be controlled such that it will be much smaller than T at any accessible temperature. The existence of a finite resistance limit such as that found in these systems which exhibit superconducting behavior is unusual, as the scaling theory of localization would predict all electrons in two-dimensional systems to be localized, and thus all films insulating in limit $T\rightarrow 0$ unless they become superconducting.

An interesting question is whether the scaling behavior described above is a distinctive feature of superconducting systems, or is a general property found even in two-dimensional nonsuperconducting systems if they are examined at a comparable level of detail. This issue was addressed by studying films of Pd, which did not exhibit superconductivity.[50] Palladium films have a number of unique properties that make them particularly suitable for study. In particular, they wet ceramic and glass substrates extremely well, and thus can be made so thin that they are easily two-dimensional. In this study, measurable conductances, e.g., sheet resistances $R<10G\ \Omega$ at 4 K, were found at a thickness of about 8.8 Å. Palladium films grown on liquid-helium temperature substrates are also amorphous. These two properties ensure that Pd film systems can be made homogeneous, exhibiting disorder only at atomic length scales. An analysis of data for the conductance of sequentially deposited Pd films showed that in a manner similar to that found for superconducting films $\sigma=\sigma(T,d)=\sigma(T/T_0(d))$, where d is the film thickness. On the other hand the scaling functions for the films of superconducting and nonsuperconducting metals were different. Within the experimental parameter range for insulating films of the superconducting sequences, in the limit of $T/T_0(d)\rightarrow 0$, $\sigma\approx\exp(-T_0/T)$, while for nonsuperconducting sequences, the corresponding limiting behavior was $\sigma\approx\exp[-(T_0/T)^{1/2}]$. Although the electrical conductivities of all insulating films of superconducting materials, Bi, Pb, and Al, fell into a single scaling curve, additional parameters were required to achieve a similar collapse for different sequences of Pd films. The most important difference was that the scaling parameters $T_0(d)$, were very different functions of thickness or Boltzmann conductance. In the case of Pd they fell to zero over an extended range of thicknesses or Boltzmann conductances, exponentially, as metallic behavior was approached. This must be contrasted with the nonexponential decay of T_0 with either sheet resistance or thickness in nonsuperconducting Bi, Pb, and Al films as the superconducting state was approached.

IV. THE INSULATOR-SUPERCONDUCTOR TRANSITION AND THE BOSON HUBBARD MODEL

The analysis presented above strongly suggests that the scaling of electrical conductivities observed in films of superconducting materials Bi, Pb, and Al can be related to a phase transition at zero temperature. It has been suggested that this transition is an insulator-superconductor transition driven by quantum rather than thermal fluctuations. In this section we will connect the empirical scaling approach described in Sec. III with a scaling analysis proposed in the context of the boson Hubbard model.[1,51]

It is important to note the difference between the usual scaling analysis and the empirical one described in the previous section. When a scaling analysis is carried out in a conventional manner, independent measurements are made to determine the critical exponents, and after finding them, the data is collapsed onto a universal curve. In the empirical approach the opposite is done. First the data is collapsed empirically onto a scaling curve. The critical exponents are then deduced from the dependence on a control parameter of the scaling parameter used to collapse the data.

Fisher and co-workers[1,51] have argued that a disordered superconductor can be modeled as a collection of interacting charged ($2e$) bosons moving in a two-dimensional random potential, i.e., a boson Hubbard model. The bosons correspond to Cooper pairs and are assumed to exist on *both* sides of the insulator-superconducting transition. At low enough temperatures, below the "bulk" superconducting transition temperature, and in the critical regime of the insulator-superconductor transition, the dc resistance R can be written as $R=(h/4e^2)Q[b\delta/T^{1/\nu z}]$, where Q is a universal function, δ is a control parameter, and b is nonuniversal constant. The parameter δ, in the case of the field-

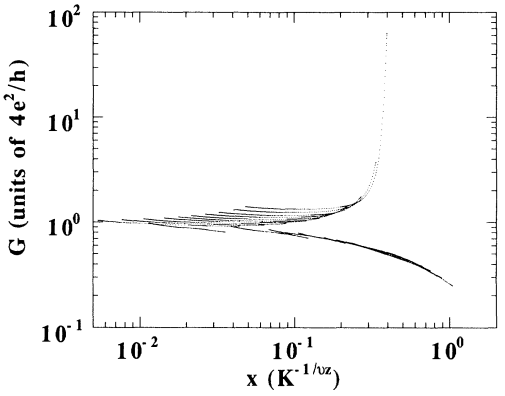

FIG. 18. Conductance G vs x for 20 Bi films in the vicinity of the insulator-to-superconductor transition. The quantity $x=|\delta/T^{1/\nu z}|$, where δ, ν, and z are defined in the text. The critical point corresponds to $x=0$. For insulating and superconducting films the values of νz are taken to be 2.8 and 1.5, respectively.

induced transition is of the form $\delta=|H-H_c|$, where H is the applied field and H_c is the critical field. In the case of the zero-field transition δ can be taken to be either $|d-d_c|$, or $|R-R_0|$, where d is the film thickness, d_c is the critical film thickness, R is the sheet resistance measured at high temperatures, and R_0 is the critical sheet resistance. One can relate the empirical scaling analysis of Sec. III to the present discussion by noting that the variation of the conductance with temperature $G=G(T/T_0^{I,S})$, with $T_0^{I,S}\approx\delta^{i,s}$ is equivalent to the expression for the resistance given above if one makes the identification of the exponents i and s with the product νz. Having determined i and s from the dependence of T_0 on δ, one can then replot the data in the scaled form shown in Fig. 18 using $\nu z=2.8$ for insulating films and $\nu z=1.5$ for superconducting ones. As one can see all of the data do not collapse onto curves corresponding to positive and negative δ. The collapse of this range of data is much poorer if one chooses $\nu z=1.5$ for both superconducting and insulating films. Although the same caveats relating to the asymptotic limit in the discussion relating to Fig. 17 hold here, these results exhibit the connection between the empirical scaling approach of Sec. III and that suggested in the context of the boson Hubbard model.

V. CONCLUSIONS AND DISCUSSION

Sets of films of superconducting materials grown on amorphous Ge substrates were investigated as a function of thickness, a study facilitated by the possibility of semicontinuous variation of film thickness using the technique of successive deposition at low temperatures. In the $T\rightarrow 0$ limit, the films were either insulating or superconducting. In each instance a separatrix between superconducting and insulating films could be found. For amorphous Bi films this separatrix corresponded to a film with a normal sheet resistance $R_0=(6.42\pm0.2)$kΩ, a number very close to quantum resistance for pairs, $h/4e^2=6455$ Ω. For films of Pb and Al the separatrix corresponded to films with normal-state resistances of 9.94 ± 0.4 kΩ and 18.6 ± 1.7 kΩ, respectively. The temperature-dependent electrical conductances of the sets of films could be scaled with a single parameter with a functional form given by $G=G(T/T_0^{I,S})$, where T_0^I and T_0^S were the values of the scaling parameters on the insulating and superconducting sides of the transition.

In every instance substantially more scatter was found in the scaling of the Pb and Al films than in the case of Bi. Despite this, the scaling curves for all three materials, at least on the insulating side collapsed onto a single curve, without any adjustable parameters, and with an asymptotic resistance limit given by that found for the Bi sequence. This strongly suggests the existence of a universal scaling curve with a universal critical resistance defined by this asymptotic value. In the Pb and Al sequences superconductivity develops before the asymptotic limit of the scaling function is achieved. It is possible this may actually be the onset of *local* superconductivity due to mesoscale inhomogeneities in the Pb and Al films, with the local resistance minima occurring at temperatures below the minimum temperature of our experiments. This hypothesis allows for the possibility that the limit $T\rightarrow 0$ resistance of the scaling function may be the same in all of the sequences. For the sequence of Al films, there was also a large gap in thickness between the last insulating and first superconducting films, suggesting that these superconducting films were not very close in their parametrization to the threshold for superconductivity.

The absence of physical and chemical inhomogeneities, or changes in the structure during the course of successive depositions would appear to be absolutely essential for the success of the scaling analysis. It would appear that only for the sequence of Bi films was there no evidence of these deleterious effects. It is important to realize that deposition onto substrates cooled to liquid-helium temperatures may not eliminate motion of atoms on the cold surface. The energy for the latter can come from the kinetic energy of the impinging atoms, from their condensation energy or from radiant heating of the substrate by a hot source. Of the three metal systems we have studied in detail, Bi, Pb, and Al, Bi has the lowest condensation energy, and lowest source temperature, and Al, the highest. Bismuth appears to follow the scaling curve to the lowest conductance before becoming superconducting, whereas Al, with the highest condensation energy and highest source temperature of the three appears to become superconducting the soonest.

The critical resistance for the insulator-superconductor transition inferred from the asymptotic limit of the universal scaling curve was close to $R_0(\approx 6.42$ kΩ). In all instances the values of T_0^I and T_0^S fell to zero as the insulator-superconductor transition was approached with an algebraic dependence on the control parameter. This is in marked contrast with a similar analysis of Pd films. The above observations on superconducting systems have been interpreted as evidence of a direct transition from

an insulator to a superconductor at zero temperature. Clearly further detailed studies are needed to more precisely define the critical regime and to find the true critical exponents.

The scaling of the insulator-to-superconductor transition has been interpreted as evidence of a quantum phase transition at zero temperature such as that described by a boson Hubbard model. In this theory, the asymptotic value of the resistance $[h/4e^2]Q(0)$ is a universal quantity. A proof of this universality has been given using the hyperuniversality assumption for quantum phase transition at zero temperature (within the Boson model) and the Kubo formula, which relates the conductivity to the superfluid density.[52] Within the boson Hubbard model, the value of the critical resistance has been shown to be precisely $h/4e^2$ only if the model is *self-dual* under charge-vortex transformation.[51,53] In this picture, charges (Cooper pairs) and vortices exchange roles on the two sides of the insulator-superconductor transition. The requirement of self-duality is a very strong constraint that may not be achievable for real films as the vortex-vortex interaction and the Coulomb interaction must have the same functional form to satisfy it. On the other hand, a sample-dependent value of the critical resistance would not be consistent with the boson Hubbard model, which predicts a universal resistance, although not its precise value, except in the case of self-duality.[51] If a marginal variable not included in the theory determined the value of the critical resistance, then the boson Hubbard model would be ruled out.[54] The scaling analysis which we have developed implies the existence of a universal value of the limiting resistance.

It is interesting to note again that within the analysis of the available experimental data, the exponents i and s differ roughly by a factor of 2. Usually critical exponents are the same on either side of the critical point. A detailed scrutiny of data very close to the critical resistance suggests that this difference may vanish, with both exponents having the value on the superconducting side, if the critical regime is sampled in a more detailed way. This will require the study of films close in their properties to the threshold, and lower temperatures. The exponents of the boson Hubbard model arise from the characteristic frequency, $\Omega \sim \delta^z$, and characteristic length $\xi_B \sim \delta^{-\nu}$ associated with the transition. They should be the same on the two sides of the transition. In the context of the present work, as mentioned above, the phenomenological parameters $T_0^{I,S}$ vanish as $T_0^{I,S} \sim \delta^{z\nu}$. It has been argued that the dynamical critical exponent z should be unity for a charged system.[55] Real-space renormalization calculations[56] seem to confirm this result and furthermore suggest $z\nu \approx 1.4$. The latter compares favorably with the result from fitting on the superconducting side.

There is a general question of the applicability of the particular form of boson mode that should be addressed. It has been shown that the Josephson-junction array Hamiltonian,[57] which is presumably the correct model for granular films, can be mapped onto a boson Hubbard model. This mapping is precise if the fluctuations of the amplitude of the order parameter on individual grains are small.[58] When these fluctuations are large, another model may be needed although it is possible that it belongs to the same universality class as the boson Hubbard model. For homogeneous films, the Josephson-junction array model may be inappropriate because of the absence of well-defined superconducting grains. In this case, however, one may still envision localized states of Cooper pairs, which are constrained spatially, as effective grains.[59] These localized pairs could then be coupled with nearby pairs via some effective Josephson coupling. In this scenario, the boson model might still be applicable following arguments similar to those used for granular superconducting films.

The boson Hubbard model requires the existence of Copper pairs on both the superconducting and insulating sides of the transition. This is a natural assumption for the superconducting side. It may also be natural to describe the pairs as bosons on the superconducting side as the coherence length is reduced in disordered films.[60] For these Cooper pairs, the only relevant energy scale would be the energy gap. Therefore, T_0^S could be related to the gap or superconducting transition temperature. T_0^I would be the corresponding quantity on the insulating side if pairs also existed there. Then the fact that both T_0^S and T_O^I fall to zero at the superconductor-insulator transition, and that T_O^I is very small near the transition, may make it possible to reconcile the present analysis of the transition with recent tunneling studies. In the latter, the superconducting gap was found to fall to zero with T_c, as the superconductor-insulator transition was approached from the superconducting side, and was not measurable on the insulating side.[61]

For insulating films there may be further complications. According to the scaling function we have found, at sufficiently low temperatures, the electrical conductivity scales continuously to the behavior, exponential in temperature, of the thinnest films, even for films that are close in their properties to the onset of superconductivity and, which exhibit logarithmic temperature dependences at high temperatures. Thus the low-temperature behavior of the thicker films should involve the same physics as the general behavior of the thinner ones. Although it would not be unreasonable for the thicker insulating films to have Cooper pairs, in the case of the thinnest films, even local pairing should not be possible as the strong long-range Coulomb repulsion would overcome any attractive interaction. This, together with the scaling function, which links the low-temperature behavior of thicker films to the behavior of the thinnest films, suggest that at sufficiently low temperatures all films will be Fermi rather than Bose insulators. It is an open experimental question as to whether a transition between these two types of insulators actually occurs as a function of temperature or sheet resistance. There is evidence of such a transition in Hall effect studies of In_2O_3 in varying magnetic fields.[62]

Measurements of films grown on a-Ge may have an additional complication related to the discussion given just above. Although Hall studies have not been carried out, it is very likely that the average electron density in these systems is much less than that of metals. Such is indeed the case for In_2O_3 films. If reduced carrier densities

characterize both of these systems, then it is possible that the pairing leading to superconductivity is real space rather than momentum space pairing.[61] Real-space pairs might behave more like composite bosons, which exhibit no spatial overlap of the wave functions of different pairs, in contrast with conventional momentum space or Cooper pairs in which there is substantial spatial overlap. A dependence of the carrier concentration on thickness for ultrathin films, or a variation from material to material would have important consequences.

The temperature dependence of the resistive tails of superconducting films with parameters placing them close to the threshold is Arrhenius in character, i.e., $R \approx \exp[-T_0^S/T]$. For thicker films one might have expected that the resistive tails would have been described by the Kosterlitz-Thouless-Berezinskii (KTB) model.[23] This was not found, although the high-temperature behavior of the resistance of these films could be fit by the Aslamazov-Larkin theory[63] in a conventional manner. In the work on the field-induced superconductor-insulator transition in amorphous composite In_2O_3 films,[43] zero-field resistive transitions could be fit rather accurately by the KTB model. Similarly, in studies of quench-condensed Hg/Xe films carried out a number of years ago, the KTB model provided an excellent account of the data for the superconducting transition.[64] The films, which were studied in this work, had thicknesses that were far less than 100 Å, in contrast with thicknesses in 100–200 Å range for both In_2O_3 and Hg/Xe films. We conjecture that the inability of the KTB model to represent data is a consequence of quantum effects being dominant for films close to the threshold even in zero magnetic field. In the context of the phase diagram of Ref. 51, the ultrathin films of the type studied in this work, in contrast with amorphous composite In_2O_3 and Hg/Xe films, would undergo superconducting transitions in zero magnetic field at positions on the phase diagram very close to the end point of the KTB phase boundary. In this regime crossover effects between the KTB and quantum universality classes might be expected. Such crossover effects could lead to resistive transitions with temperature dependences different from those of the KTB model. They might also lead to changes in values of the critical exponents such as discussed above. Clearly more detailed studies are needed to resolve this issue.

Further experimental studies could resolve a number of important issues raised by the present work. Future work could include studies of structure, Hall measurements to determine carrier concentrations, tunneling studies to determine the nature of the states of both superconducting and insulating films, studies of electrical conductivity at ultralow temperatures, in films with parameters very close to the insulator-superconductor transition, and measurements of the Aharonov-Bohm effect of insulating films. The latter might reveal whether the charge carriers in the insulating state were pair or single-particle excitations.[65] In addition, study of the field-induced transition in samples close to the threshold would reveal the nature of the phase diagram and permit a comparison of the zero-field and field-induced transitions, which although similar, do not have the same symmetry.

ACKNOWLEDGMENTS

The authors would like to thank a number of individuals who contributed significantly to this work at various stages. Professor J. W. Halley made some important suggestions regarding the one-parameter scaling approach. Dr. K. McGreer was heavily involved in the early stage of some of the data analysis. We would also like to thank C. Castellani, S. Chakravarty, C. Dasgupta, J. Duan, M. P. A. Fisher, S. M. Girvin, L. I. Glazman, R. E. Glover, J. Kakalios, S. Kivelson, D. Khmel'nitskii, A. J. Leggett, M. Ma, T. V. Ramakrishnan, B. Shklovskii, X-Q. Wang, P. B. Weichman, X-G. Wen, and L. Zhang for useful discussions. This work was supported by the Low-Temperature Physics program of the National Science Foundation under Grant No. NSF/DMR-9001874.

*Present address: Dept. of Physics, University of Colorado, Campus Box 390, Boulder, CO 80309.

†Present address: Dept. of Physics, Chalmers Technical University, S-412 96 Göteborg, Sweden.

[1]Matthew P. A. Fisher, G. Grinstein, and S. M. Girvin, Phys. Rev. Lett. **64**, 587 (1990).

[2]T. Wang, K. M. Beauchamp, D. D. Berkely, J-X. Liu, J. Zhang, and A. M. Goldman, Phys. Rev. B **43**, 8623 (1991).

[3]G. T. Seidler, T. V. Rosenbaum, and B. W. Veal, Phys. Rev. B **45**, 10 162 (1992).

[4]J. M. Graybeal and M. R. Beasley, Phys. Rev. B **29**, 4167 (1984).

[5]H. R. Raffy, R. B. Laibowitz, P. Chaudhari, and S. Maekawa, Phys. Rev. B **28**, 6607 (1983); S. J. Lee and J. B. Ketterson, Phys. Rev. Lett. **64**, 3078 (1990).

[6]A. F. Hebard and M. A. Paalanen, Phys. Rev. Lett. **65**, 927 (1990).

[7]M. Strongin, R. S. Thompson, O. F. Kammerer, and J. E. Crow, Phys. Rev. B **2**, 1078 (1971).

[8]R. C. Dynes, J. P. Garno, and J. M. Rowell, Phys. Rev. Lett. **40**, 479 (1978).

[9]A. I. Shal'nikov, Zh. Eksp. Teor. Fiz. **10**, 630 (1940); Nature (London) **142**, 74 (1938).

[10]W. Buckel and R. Hilsch, Z. Phys. **138**, 109 (1954); W. Buckel, *ibid.* **138**, 1360 (1954).

[11]E. Abrahams, P. W. Anderson, G. Licciardello, and T. V. Ramakrishnan, Phys. Rev. Lett. **42**, 673 (1979).

[12]W. Kohn, Phys. Rev. **133A**, 171 (1964).

[13]D. Forster, *Hydrodynamic Fluctuations, Broken Symmetry, and Correlation Functions* (Benjamin, New York, 1975), p. 290; G. Toulouse, in *Recent Developments in Gauge Theories,* edited by G. t'Hooft, C. Itzykson, A. Joffe, H. Lehmann, P. K. Mitter, I. M. Singer, and R. Storer (Plenum, New York, 1980), p. 331.

[14]P. C. Hohenburg, Phys. Rev. **158**, 383 (1967).

[15]S. Maekawa and H. Fukuyama, J. Phys. Soc. Jpn. **51**, 1380 (1982).

[16]P. W. Anderson, K. A. Muttalib, and T. V. Ramakrishnan, Phys. Rev. B **28**, 117 (1983).

[17]P. W. Anderson, J. Phys. Chem. Solids **11**, 26 (1957).

[18]A. M. Finkel'shtein, Pis'ma Zh. Eksp. Teor. Fiz. **45**, 37 (1987) [JETP Lett. **45**, 46 (1987)].
[19]P. A. Lee and T. V. Ramakrishnan, Rev. Mod. Phys. **57**, 287 (1985).
[20]N. F. Mott, J. Non-Cryst. Solids **1**, 1 (1968).
[21]G. Bergmann, Phys. Rep. **27**, 159 (1976).
[22]R. E. Glover III, Phys. Lett. **25A**, 542 (1967).
[23]For a review, see J. E. Mooij, in *Percolation, Localization, and Superconductivity,* edited by A. M. Goldman and S. Wolf (Plenum, New York, 1984), p. 433.
[24]R. C. Dynes, A. E. White, J. M. Graybeal, and J. P. Garno, Phys. Rev. Lett. **57**, 2195 (1986).
[25]J. M. Valles, Jr., R. C. Dynes, and J. P. Garno, Phys. Rev. B **40**, 6680 (1990).
[26]D. B. Haviland, Y. Liu, and A. M. Goldman, Phys. Rev. Lett. **62**, 2180 (1989); Y. Liu, K. A. McGreer, B. Nease, D. B. Haviland, G. Martinez, J. W. Halley, and A. M. Goldman, *ibid.* **67**, 2068 (1991).
[27]B. G. Orr, H. M. Jaeger, A. M. Goldman, and C. G. Kupeer, Phys. Rev. Lett. **56**, 378 (1986); H. M. Jaeger, D. B. Haviland, B. G. Orr, and A. M. Goldman, Phys. Rev. B **40**, 182 (1989).
[28]L. J. Geerligs, M. Peters, L. E. M. de Groot, A. Verbruggen, and J. E. Mooij, Phys. Rev. Lett. **63**, 326 (1989).
[29]Y. Liu, B. Nease, and A. M. Goldman, Phys. Rev. B **45**, 10 143 (1992).
[30]L. I. Glazman and N. Ya Fogel', Fiz. Nizh. Temp. **10**, 95 (1984) [Sov. J. Low Temp. Phys. **10**, 51 (1984)].
[31]Y. Liu, D. B. Haviland, L. E. Glazman, and A. M. Goldman, Phys. Rev. Lett. **68**, 2224 (1992).
[32]B. G. Orr and A. M. Goldman, Rev. Sci. Instrum. **56**, 1288 (1985).
[33]N. Kurti and F. E. Simon, Proc. R. Soc. London Ser. A **151**, 610 (1935).
[34]B. Weitzel and H. Micklitz, Phys. Rev. Lett. **66**, 385 (1991).
[35]W. Buckel, Z. Phys. **154**, 474 (1959).
[36]W. Buckel and J. Wittig, Phys. Lett. **17**, 187 (1965).
[37]G. Bergmann, Z. Phys. **255**, 76 (1972).
[38]Y. Liu, Ph.D. thesis, University of Minnesota, 1991 (unpublished).
[39]A. Miller and E. Abrahams, Phys. Rev. **120**, 745 (1960).
[40]D. C. Licciardello and D. J. Thouless, Phys. Rev. Lett. **35**, 1475 (1975).
[41]I. S. Shlimak, in *Hopping and Related Phenomena,* edited by H. Fritzsche and M. Pollak (World Scientific, Singapore, 1990), p. 49.
[42]B. I. Shklovskii and A. L. Efros, *Electronic Properties of Doped Semiconductors* (Springer-Verlag, Berlin, 1984).
[43]A. F. Hebard and M. A. Paalanen, Phys. Rev. Lett. **65**, 927 (1990).
[44]P. G. de Gennes, Rev. Mod. Phys. **36**, 225 (1964).
[45]J. Simonin, Phys. Rev. B **33**, 7830 (1985).
[46]D. B. Haviland, Ph.D. thesis, University of Minnesota, 1989 (unpublished).
[47]R. A. Ferrell and C. J. Lobb (unpublished).
[48]B. G. Orr, H. M. Jaeger, and A. M. Goldman, Phys. Rev. Lett. **53**, 2046 (1984).
[49]A. Möbius, H. Vinzelberg, C. Gladan, A. Heinrich, D. Elefant, J. Schumann, and G. Zies, J. Phys. C **18**, 3337 (1985), and references cited therein.
[50]Y. Liu, B. Nease, K. A. McGreer, and A. M. Goldman, Europhys. Lett. **19**, 409 (1992).
[51]M-C. Cha, M. P. A. Fisher, S. M. Girvin, Mats Wallin, and A. Peter Young, Phys. Rev. B 44, 6883 (1991).
[52]K. Kim and P. B. Weichman, Phys. Rev. B **43**, 13 583 (1991).
[53]X. G. Wen and A. Zee, Int. J. Mod. Phys. B **4**, 437 (1990).
[54]S. Kivelson (private communication).
[55]M. P. A. Fisher, P. B. Weichman, G. Grinstein, and D. S. Fisher, Phys. Rev. B **40**, 546 (1989).
[56]L. Zhang and M. Ma, Phys. Rev. B **45**, 4855 (1992).
[57]S. Doniach, Phys. Rev. B **24**, 5063 (1981).
[58]P. B. Weichman, in *Recent Progress in Many-Body Theories,* edited by T. L. Ainsworth, C. E. Campbell, B. E. Clements, and E. Krotschek (Plenum, New York, 1992), Vol. 3, p. 361.
[59]M. Ma, B. I. Halperin, and P. A. Lee, Phys. Rev. B **34**, 3136 (1986).
[60]M. Randeria, J-M. Duan, and L-Y. Shieh, Phys. Rev. B **41**, 327 (1990).
[61]J. M. Valles, Jr., R. C. Dynes, and J. P. Garno, Phys. Rev. Lett. **69**, 3567 (1992).
[62]M. A. Paalanen, A. F. Hebard, and R. R. Ruel, Phys. Rev. Lett. **69**, 1604 (1992).
[63]L. G. Aslamazov and A. I. Larkin, Phys. Lett. **26A**, 238 (1968).
[64]K. Epstein, A. M. Kadin, and A. M. Goldman, Phys. Rev. Lett. **47**, 534 (1980); Phys. Rev. B **27**, 6691 (1983).
[65]Kivelson and Spivak have suggested than an observation of $hc/4e$ Aharonov-Bohm oscillations would not imply charge $2e$ carriers. See, S. A. Kivelson and B. Z. Spivak, Phys. Rev. B **45**, 10 490 (1992).